Photoactive Thermoplastic Elastomers of Azobenzene-Containing Triblock Copolymers Prepared through Atom Transfer Radical Polymerization

Li Cui,[†] Xia Tong,[†] Xiaohu Yan,[‡] Guojun Liu,[‡] and Yue Zhao*,[†]

Département de Chimie, Université de Sherbrooke, Sherbrooke, Québec, Canada J1K 2R1, and Centre de recherche en science et ingénierie des macromolécules (CERSIM), Université Laval, Québec, Canada G1K 7P4, and Department of Chemistry, University of Calgary, Calgary, Alberta, Canada T2N 1N4

Received May 20, 2004; Revised Manuscript Received July 21, 2004

ABSTRACT: Atom transfer radical polymerization (ATRP) was used to prepare a new series of ABA triblock copolymers that are photoactive thermoplastic elastomers. The samples synthesized have the same rubbery midblock of poly(*n*-butyl acrylate) (PnBA) but differ in the degree of polymerization of the end blocks of a methacrylate-based azobenzene-containing side-chain liquid crystalline polymer (Azo-SCLCP). The coupling between elasticity, liquid crystallinity and photoactivity imparts interesting features to this type of thermoplastic elastomers. When the solution-cast film is stretched at $T > T_g$ of the Azo-SCLCP whose microdomains act as physical cross-links, in contrast to conventional thermoplastic elastomers (such as styrene−butadiene−styrene triblock copolymer) that lose the elasticity, liquid crystalline microdomains can support part of the elastic extension of PnBA chains and, in the same time, deform to result in a long-range orientation of azobenzene mesogens. The liquid crystal orientation is retained in the relaxed film at $T < T_g$, which creates a thermoplastic elastomer whose glassy microdomains contain oriented azobenzene mesogens. Moreover, the reversible trans−cis photoisomerization of the azobenzene chromophore can be used to modulate the mechanically induced orientation.

Introduction

In recent years much effort has been devoted to azobenzene-containing polymers (azo polymers) due to their interesting properties related to the reversible photoisomerization between the trans and cis isomers of the chromophore.[1] The azo polymers studied include amorphous polymers,[1−3] liquid crystalline polymers,[1,4−7] block copolymers,[8,9] and dendrimers.[10] They have potential for applications ranging from optical storage to optical actuators.[1,2,11,12] One particular type of azo polymers is the thermoplastic elastomer we have investigated recently.[13−16] Through radical polymerization of a methacrylate or acrylate-based monomer bearing an azobenzene group in solution with a dissolved styrene−butadiene−styrene (SBS) triblock copolymer, the azobenzene-containing side-chain liquid crystalline polymer (Azo-SCLCP) could be grafted to the polybutadiene midblock of SBS, and the resultant material is an azo thermoplastic elastomer that displays interesting features. We showed that solution-cast films could be stretched at room temperature to induce orientation of azobenzene mesogens and that diffraction gratings could be recorded on the stretched film with mechanically tunable diffraction angle and efficiency through the elastic deformation of the film.[15,16] Although the content of Azo-SCLCP could be varied from about 8 to 30 wt %, the preparation method lacked control in that important parameters such as the length and number of the azo polymer grafts were unknown. It is thus of interest to develop azo thermoplastic elastomers of novel structures using other synthetic methods.

In this paper we report the synthesis of new azo thermoplastic elastomers that are ABA-type triblock copolymers, with the A end blocks being an Azo-SCLCP and the B midblock a rubbery polymer. In a previous work,[17] we prepared diblock copolymers composed of polystyrene and an Azo-SCLCP by atom transfer radical polymerization (ATRP) and used some diblock copolymers as model systems to investigate the confinement effects of microphase-separated domains on the photoalignment, photochemical phase transition, and thermochromic behaviors of the Azo-SCLCP.[18] In the present study, the ATRP method was applied to prepare the azo triblock copolymers. The end blocks are the same Azo-SCLCP, namely, poly{6-[4-(4-methoxyphenylazo)phenoxy]hexyl methacrylate}, while the rubbery midblock chosen is poly(*n*-butyl acrylate) (PnBA) that has been used to make thermoplastic elastomers with poly(methyl methacrylate) end blocks through ATRP.[19] As will be shown, the azo triblock copolymers are thermoplastic elastomers in which the microphase-separated domains of the Azo-SCLCP act as the cross-links supporting the extension of PnBA chains. As compared to conventional systems such as SBS, the new azo elastomer has some interesting properties due to the coupling between elasticity, liquid crystallinity, and photoactivity.

Experimental Section

1. Synthesis. a. Materials. THF was refluxed with sodium and distilled. *n*-Butyl acrylate (Aldrich) was distilled with 2,6-di(*tert*-butyl-4-methyl)phenol as inhibitor before use. The other commercially available chemicals were used without further purification. Methods reported in the literature were used to synthesize the azobenzene monomer,[20] 6-[4-(4-methoxyphenylazo)phenoxy]hexyl methacrylate, and tris[2-(dimethylamino)ethyl]amine (Me_6TREN).[21] Details on the preparation of triblock copolymers through ATRP are given below.

b. Preparation of 1,1′-Biphenyl-4,4′-bis(2-bromoisobutyrate) (Dibromo Initiator). 4,4′-Biphenol (0.47 g, 2.5

[†] Université de Sherbrooke.
[‡] University of Calgary.
* Corresponding author. E-mail: yue.zhao@usherbrooke.ca.

10.1021/ma048995j CCC: $27.50 © 2004 American Chemical Society
Published on Web 08/27/2004

Table 1. Characteristics of Synthesized Polymers

sample	azo content[a] (wt %)	conv[b] (%)	M_n (GPC)	M_w/M_n (GPC)	M_n (NMR)[c]	phase transitions[d] (°C)	ΔH_{S-N}[e] (J/g)	ΔH_{N-I}[e] (J/g)
PAzo	100		21K	1.25		g74S92N129I	1.98	3.69
P1	50.5	52	82K	1.93	32.1K−62.9K−32.1K	g_1−37 $g_2$71S79N116I	1.66	1.95
P2	34.5	83	119K	1.26	16.6K−62.9K−16.6K	g_1−36 $g_2$72S81N115I	1.03	0.72
P3	28.3	41	108K	1.24	12.4K−62.9K−12.4K	g_1−36 $g_2$68S77N114I	0.88	0.61
P4	25.4	39	99K	1.22	10.7K−62.9K−10.7K	g_1−36 $g_2$67S73N113I	0.80	0.41
P5	20.3	46	93K	1.25	8.0K−62.9K−8.0K	g_1−36 $g_2$66S74N113I	0.61	0.40
P6	19.0	34	89K	1.14	7.4K−62.9K−7.4K	g_1−35 $g_2$64S77N114I	0.39	0.26
Br−PnBA−Br	0		62.9K	1.12		g−37I		

[a] Determined from ^{1}H NMR. [b] Measured from ^{1}H NMR. [c] Using GPC-determined central block. [d] g = glass transition; S = smectic; N = nematic; I = isotropic phase. [e] With respect to the liquid crystalline azo polymer block.

mmol), triethylamine (0.55 g, 5.5 mmol), and THF (10 mL) were added in a 25 mL flask. Bromoisobutyryl bromide (1.27 g, 5.5 mmol) was added dropwise under stirring. The reaction was continued at room temperature overnight. Afterward, the mixture was poured into water, and a white solid precipitated. After filtration and recrystallization in ethanol, about 1 g of white pallet crystals was obtained. ^{1}H NMR (300 MHz, $CDCl_3$) δ: 2.1 (s, 12H), 7.20 (d, 4H), 7.6 (d, 4H).

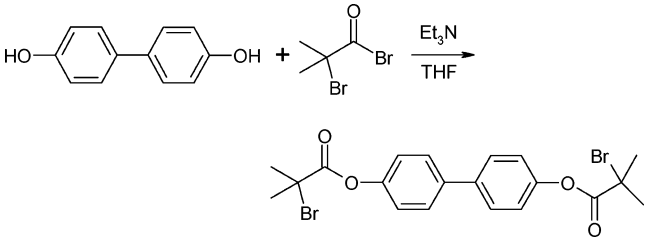

c. Preparation of Br−Poly(*n*-butyl acrylate)−Br (Br−PnBA−Br, Macroinitiator). In a Schlenk flask, *n*-butyl acrylate (3.2 g, 25 mmol), Me_6TREN (11.5 mg, 0.05 mmol), and CuBr (7.1 mg, 0.05 mmol) were mixed and stirred for 10 min. 1,1′-Biphenyl-4,4′-bis(2-bromoisobutyrate) (24 mg, 0.05 mmol) was then added. The mixture was immediately frozen in using liquid nitrogen, and a vacuum was applied. After several freeze−thaw cycles, the flask was sealed under vacuum and put in an oil bath at 20 °C for 6 h. The content was dissolved in THF and passed through an alumina column to remove the metal complex. After being concentrated, the THF solution was precipitated in methanol. The purification by precipitation was repeated several times. The final product was dried at 50 °C in a vacuum oven. M_n = 62 900 and M_w/M_n = 1.12 (GPC).

d. Preparation of Triblock Copolymers. The synthesis of P3 (acronym in Table 1) is given as an example. A round-bottom flask with a stir bar was charged with 225 mg of Br−PnBA−Br (macroinitiator for the midblock), 258 mg of 6-[4-(4-methoxyphenylazo)phenoxy]hexyl methacrylate (azo monomer), 11 mg of Me_6TREN, and 4 mL of THF. The mixture was stirred for 20 min until a homogeneous solution was formed. Immediately after copper bromide (3 mg) was introduced in the mixture, three freeze−thaw cycles were performed. The flask was sealed in the frozen state under vacuum and put in an oil bath at 60 °C for 6 h. Conversion of azo monomer, as determined by ^{1}H NMR, was about 41% (Table 1). The reaction mixture was dissolved in THF and passed through an alumina column to remove inorganic salts. The solution was then concentrated and precipitated in methanol repeatedly to purify the product. M_n = 108 400 and M_w/M_n = 1.24 (GPC).

e. Preparation of Poly{6-[4-(4-methoxyphenylazo)-phenoxy]hexyl methacrylate} (Azo-SCLCP). Experimental details on the synthesis of the azobenzene homopolymer (PAzo in Table 1) were already reported.[17] CuBr complexed with *N*,*N*,*N*′,*N*′,*N*″-pentamethyldiethylenetriamine was used as catalyst and ethyl bromoisobutylate as initiator.

2. Preparation of Solution-Cast Films. To prepare the free-standing films of azo triblock copolymers used for mechanical stretching, orientation measurement, and grating recording, the sample was dissolved in THF with a concentration of 4%, and the film was prepared by casting the homogeneous solution on a Teflon plate. After most solvent was slowly evaporated at ambient conditions for 2 days, the film was further dried in a vacuum oven at 50 °C for another 2 days. The films had a thickness of about 30−50 μm before stretching. The SBS films used for comparative study were prepared using the same procedure. The SBS sample was purchased from Aldrich (∼30 wt % of PS, M_w = 184 000 and M_w/M_n = 1.1).[13]

3. Characterizations. ^{1}H NMR spectra were recorded on a Bruker spectrometer (300 MHz, AC 300). Molecular weights and polydispersities were measured by gel permeation chromatography (GPC) using a Waters system equipped with a refractive index and a photodiode array detector. THF was used as eluent (elution rate: 0.5 mL/min) and polystyrene standards used for calibration. Textures were observed under a Leitz DMR-P polarizing optical microscope with an Instec hot stage. Phase transition temperatures were measured using a Perkin-Elmer DSC-7 differential scanning calorimeter with a heating or cooling rates of 10 °C/min. Transmission electron microscope (TEM) observations were carried out on a Hitachi H-7000 instrument, operated at 75 kV. The samples were sliced to 80 nm thick with a Leica EM SCS cryo-microtome machine operating at −80 °C and stained with RuO_4 vapor. The azo polymer block was stained because of the phenyl groups. For the orientation measurement, polarized infrared spectra were recorded on a Bomem MB-102 FTIR spectrometer with a wire-grid polarizer and a DTGS detector. Irradiation of the films was performed using an UV and visible spot curing system (Novacure 2100) combined with interference filters (10 nm bandwidth, Oriel). UV light at λ = 365 nm and visible light at λ = 440 nm were used for irradiations.

Results and Discussion

1. Synthesis and Characterization. Before reacting the azo monomer with the PnBA macroinitiator to make the azo triblock copolymer, the activity of Br−PnBA−Br was checked by extension polymerization of *n*-butyl acrylate. GPC measurements found that samples of PnBA with extended molecular weights had narrow polydispersities (<1.2), showed no bimodality, and contained little residual macroinitiator. In another experiment, styrene was polymerized by the Br−PnBA−Br macroinitiator, which gave rise to styrene−*n*-butyl acrylate−styrene triblock copolymers displaying high elasticity. These control experiments confirmed the efficient extension polymerization conditions using the Br−PBA−Br macroinitiator. Afterward, the azo monomer, 6-[4-(4-methoxyphenylazo)phenoxy]hexyl methacrylate, was polymerized using the macroinitiator, yielding the designed azo triblock copolymer. A series of samples having the same PnBA midblock and various degrees of polymerization for the Azo-SCLCP end blocks were prepared and characterized. Their acronyms and main characteristics are given in Table 1.

Different compositions for the triblock copolymer were obtained by varying the relative amounts of the azo

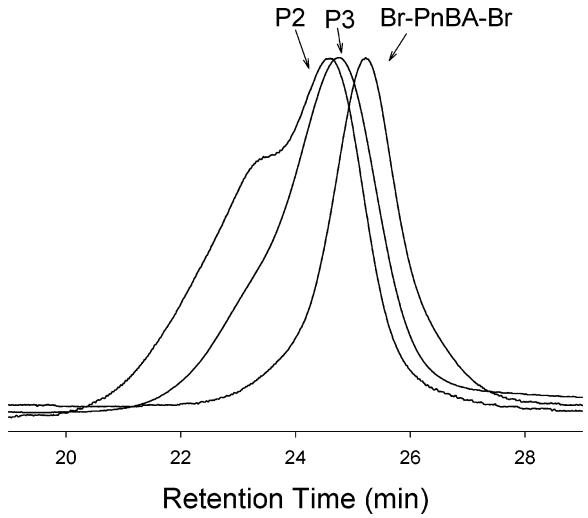

Figure 1. GPC curves of the Br−PnBA−Br macroinitiator, $\bar{M}_n = 6.3 \times 10^4$ and $\bar{M}_w/\bar{M}_n = 1.12$, and two resulting triblock copolymers with the azo polymer end blocks: P2, $\bar{M}_n = 11.9 \times 10^4$ and $\bar{M}_w/\bar{M}_n = 1.26$; P3, $\bar{M}_n = 10.8 \times 10^4$ and $\bar{M}_w/\bar{M}_n = 1.24$.

monomer and macroinitiator at similar conversions of the azo monomer (around 40%). Figure 1 shows some representative GPC curves. Comparison with the macroinitiator indicates a successful initiation and growth of the Azo-SCLCP blocks in the P3 sample. The GPC curve of P3 shows no bimodality, and although its polydispersity (1.24) is somewhat larger than that of the macroinitiator (1.12), the radical polymerization clearly took place in a controlled manner. The same situation was found for other triblock copolymers with smaller degrees of polymerization for the Azo-SCLCP blocks (P4−P6). However, P1 and P2 are different. The triblock copolymer P1, which has the highest azo polymer content around 50 wt %, has a much larger polydispersity than other samples, while in the case of P2, which was prepared with an exceptionally high conversion (83%) for the azo monomer, the GPC curve shows bimodality with the appearance of a shoulder peak on the high molecular weight side (Figure 1). It was noted that the shoulder peak corresponds to a molecular weight that is about the double of the molecular weight of the main peak, suggesting that some coupling termination reactions occurred at high conversions. Figure 2 shows the chemical structure of the azo triblock copolymer and the ^{1}H NMR spectrum of P3. From the peak assignments, the composition of the triblock copolymer could be determined and the number-average molecular weight of the Azo-SCLCP end blocks estimated (Table 1).

DSC and polarized optical microscope (POM) were utilized to characterize the phase transition temperatures of the azo triblock copolymers. Figure 3 shows the second DSC heating curves of some copolymers as well as the homopolymers, i.e., the Br−PnBA−Br macroinitiator and PAzo. The results indicate a thorough phase separation of the building blocks. Indeed, the low glass transition temperature of the PnBA macroinitiator ($T_g^1 = -37$ °C) was conserved in all the copolymers, while the Azo-SCLCP blocks display two mesophase transitions as PAzo, which is known to have a smectic A and a nematic phase.[22] The glass transition temperature of the Azo-SCLCP blocks, T_g^2, and the mesophase transitions (smectic−nematic and nematic−isotropic) appear at lower temperatures than PAzo, which is likely caused by the effect of phase-separated microdomains in the block copolymers. The range of the smectic phase in block copolymers is also reduced with the T_g^2 region apparently overlapped with the smectic−nematic phase transition endotherm, which brings uncertainty in the related data in Table 1. Interestingly, the phase transition temperatures are similar for all compositions of block copolymers within experimental errors, on both heating and cooling (cooling curves not shown). Together with the very similar T_g^1 of the PnBA block observed in all copolymers, these observations suggest that the microphase separation remained at $T > T_{ni}$, at least up to 160 °C, which was the highest temperature used. If randomization of the two polymers occurred under the used conditions, different phase transition behaviors should be observed for the block copolymers of various compositions.

The conservation of the LC phases of the Azo-SCLCP in the triblock copolymers was also observable by POM observations. Figure 4 compares the polarizing optical micrographs of P1, P2, and P3 with the homopolymer PAzo. The pictures were taken at temperatures slightly below their respective clearing temperature, T_{ni}. In contrast to PAzo, whose nematic texture can easily develop once entering the nematic phase, the appearance of birefringent textures in the block copolymer required thermal annealing of the film for at least several minutes. While PAzo displays the typical threaded texture, the apparent texture of the block copolymer looks grainy and becomes increasingly difficult to identify as the Azo-SCLCP content is decreased. In all cases, however, birefringence due to the LC phases is prominent. The absence of the threaded nematic texture is indicative of the microphase separation expected in the azo triblock copolymers because the actual LC texture inside microdomains should be difficult to view under POM. The microphase separation in the triblock copolymers was confirmed by TEM analyses. Figure 5 shows the TEM images of P1 and P3, the dark domains being the stained Azo-SCLCP. Despite the high polydispersity of P1, a lamellar morphology is clearly visible. In the case of P3 having 28% of azo polymer, as expected, cylindrical Azo-SCLCP microdomains are formed (spherical end-view in other sections was also observed).

2. Coupling between Liquid Crystallinity and Elasticity. Combining the relatively high T_g^2 near 70 °C for the Azo-SCLCP end blocks, the low T_g^1 of −37 °C for the PnBA midblock, and the thorough microphase separation between the two polymers, the conditions for thermoplastic elastomers at ambient temperatures are fulfilled. Indeed, films of triblock copolymers could readily be prepared by solution-casting followed by drying (THF was used as the solvent). After being peeled off from the substrate (Teflon plates), they could be stretched and retracted repeatedly at room temperature, corresponding to the extension and relaxation of rubbery PnBA chains interconnected and supported by the rigid Azo-SCLCP microdomains acting as cross-linking points. The achievable elastic deformation is about 250%, observed for samples containing about 30% of the azo polymer block.

Unlike the thermoplastic elastomer SBS, for which the amorphous PS plays the role of physical cross-links, it is an Azo-SCLCP that provides cross-links in our azo triblock copolymers. This coupling between the elasticity and liquid crystallinity creates an interesting situation.

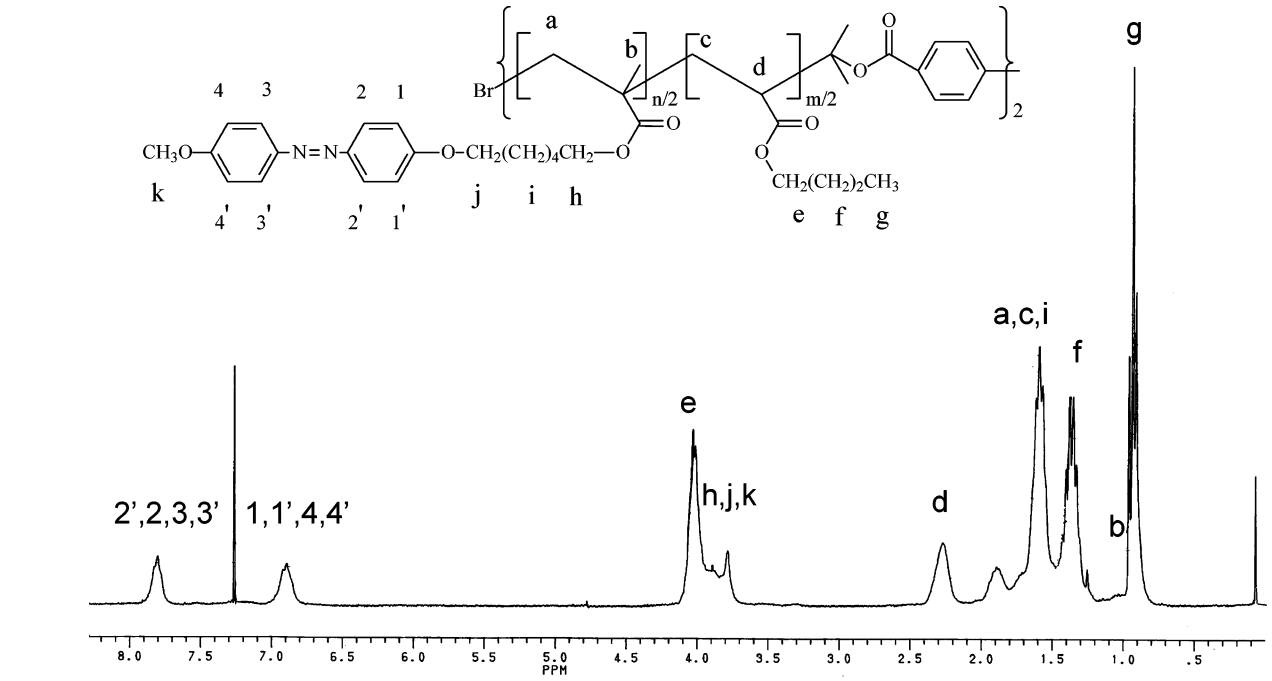

Figure 2. Chemical structure and ^{1}H NMR spectrum (sample of P3) of the azo triblock copolymer.

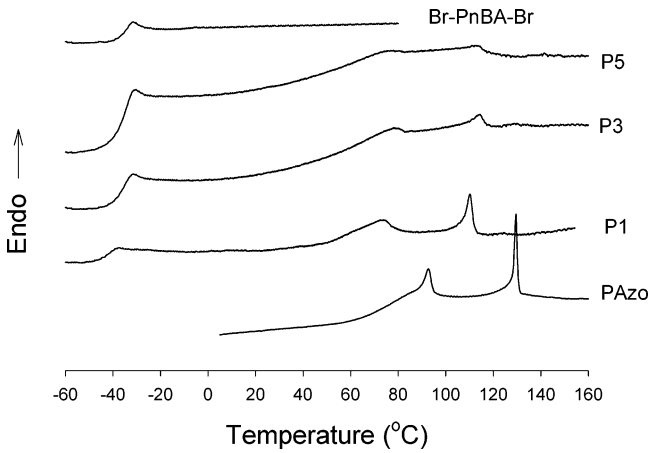

Figure 3. DSC heating curves (second scan) of the triblock copolymers and homopolymers.

When SBS is stretched at $T > T_g$ of PS, ~80 °C, the polymer is in the thermoplastic regime, where PS microdomains lose the mechanical rigidity and PB chains relax quickly during the stretching. Consequently, when the stretched film is cooled to room temperature with the mechanical force removed, there will be no elastic recovery of the film because of the total loss of the elastic orientation of PB chains. In contrast, when the azo triblock copolymer is deformed at $T > T_g$[2] of the Azo-SCLCP blocks, ~70 °C, the microdomains are in a LC phase. In response to the applied extensional force, LC microdomains may deform because of their fluid nature, but the cooperative movement of and the cohesion between the mesogenic groups could mean that the microdomains retain some rigidity to support the elastic extension of PnBA chains. The azo triblock copolymer is totally thermoplastic only at $T > T_{ni}$ (nematic–isotropic phase transition). Such an intermediate regime at $T_{ni} > T > T_g$[2] for the azo thermoplastic elastomers was observed in the experiments. For instance, films of SBS and the azo triblock copolymer P3 (initial length of 10 mm and width of 5 mm) were stretched at a rate

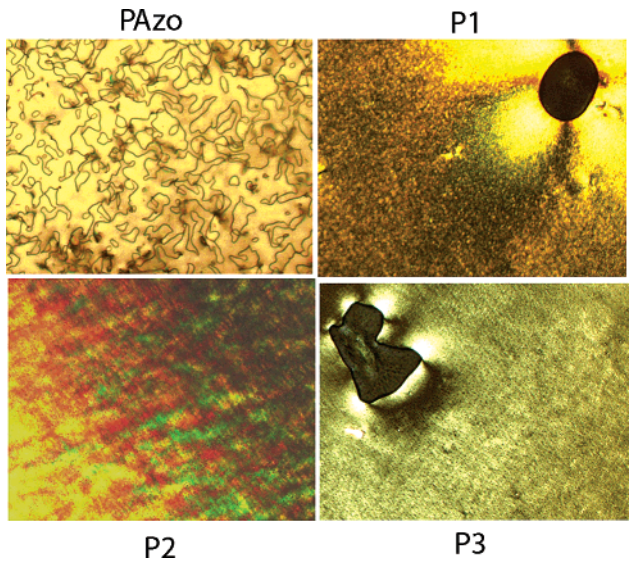

Figure 4. Polarizing optical micrographs for the homopolymer PAzo (128 °C) and three triblock copolymers: P1 (115°C), P2 (114 °C), and P3 (112 °C). Picture area: 370 μm × 300 μm.

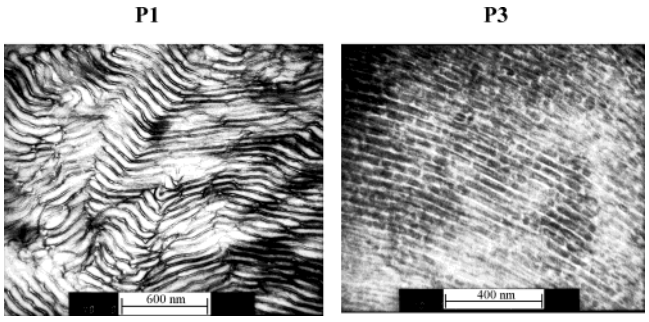

Figure 5. TEM images of two azo triblock copolymers.

of about 1 mm/s at 100 and 90 °C, respectively, i.e., ~20 °C above their respective T_g of the end blocks; immediately after stretching the films were cooled to room temperature with the mechanical force removed. The

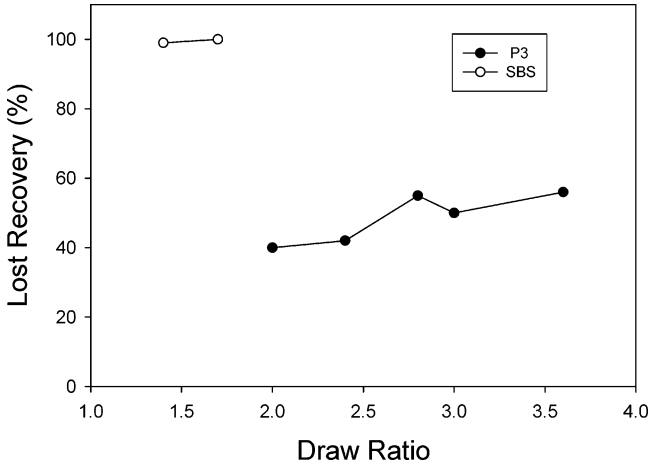

Figure 6. Lost recovery for films of SBS and the azo triblock copolymer P3 stretched at 100 and 90 °C, respectively, to various draw ratios. The elastic behavior of P3 at 90°C is indicated by the partial loss of elastic recovery of the film length.

lost recovery of the films was measured (zero lost recovery means a complete elastic recovery with the film retracting to its initial length before stretching). Plotted in Figure 6 is the measured lost recovery, defined as $(L_r - L_0)/(L - L_0)$, vs draw ratio defined as L/L_0, where L_0 is the film length before stretching, L is the length after stretching, and L_r is the residual length after relaxation at room temperature. For SBS, the lost recovery reaches 100% within experimental errors even at small strains; the film actually broke at draw ratio of 2, i.e., 100% strain. The behavior of the azo triblock copolymer P3 is clearly different. The lost recovery of the P3 film is much less important than SBS, increasing from about 40% at 100% deformation to 55% at 260% deformation. These results indicate that the film of P3 stretched at 90 °C retained part of elasticity; that is, LC microdomains slowed down the relaxation of PnBA chains during the deformation so that part of the elastic orientation remained in the stretched film after cooling to room temperature, which is responsible for the film retraction. Therefore, under the same conditions using T_g as reference temperature, the significantly higher elastic recovery and greater film deformability of the azo triblock copolymer as compared to those of SBS indicates that though less efficient than in the glassy state, LC microdomains could act as cross-links supporting part of chain extension of the rubbery midblock of PnBA. It is noted, however, that when the stretched azo triblock copolymer was held at 90 °C for more than 2 min before cooling, a complete chain relaxation of PnBA took place and the film showed no elastic recovery. Note also that for both SBS and azo triblock copolymers, when stretched at room temperature, the elastic recovery is complete, i.e., showing no lost recovery.

Polarized infrared spectroscopy was used to gain more insights into the coupling of the uniaxial deformation with the liquid crystallinity of the Azo-SCLCP through the measurement of the order parameter of azobenzene mesogenic groups inside the cylindrical microdomains acting as cross-links. The order parameter is defined as and can be determined through

$$S = (3\langle\cos^2\Theta\rangle - 1)/2 = (A_{||} - A_{\perp})/(A_{||} + 2A_{\perp})$$

where Θ is the angle between the long axis of azobenzene unit in the trans form and the stretching direction (SD); $A_{||}$ and $A_{\perp}$ are the absorbances of a characteristic absorption band of azobenzene with the infrared beam polarized parallel and perpendicular, respectively, to SD. The equation holds when the transition moment of the vibration mode considered is parallel to the long axis of trans azobenzene, which is the case for the phenyl C−C stretching bands near 1500 and 1600 cm^{-1}.[23] The order parameter S thus measures the average molecular orientation of all azobenzene groups in the sample and can have values between −0.5 and 1. $S = 1$ means perfect orientation of all azobenzene groups along SD, while $S = -0.5$ indicates perfect orientation perpendicular to SD. The absence of any long-range molecular orientation of azobenzene mesogens will lead to $S = 0$, which is the case for Azo-SCLCPs having a polydomain texture.[13] It should be emphasized that the molecular orientation of azobenzene mesogens revealed by polarized infrared spectroscopy may or may not be related to mechanically induced changes in the nematic state of order or the hexagonal order of cylindrical microdomains usually found in this type of triblock copolymers. This has not been investigated in the present work and will be the subject of future studies.

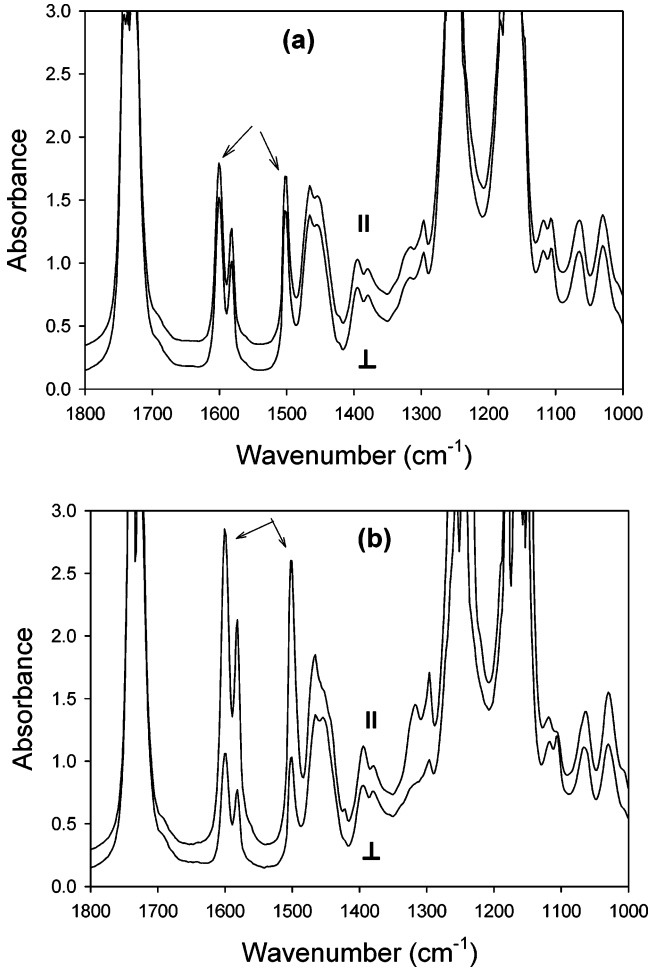

Figure 7. Polarized infrared spectra for films of the azo triblock copolymer P3 under a strain of 200%: (a) stretched at room temperature and (b) stretched at 90 °C before cooling to room temperature. The spectra were taken with the infrared beam polarized parallel (||) and perpendicular (⊥) to the stretching direction.

Figure 7 shows polarized infrared spectra for films of P3 stretched to a strain of 200% at room temperature ($T < T_g$[2]) and at 90 °C ($T_{ni} > T > T_g$[2]) followed by cooling

to room temperature. The spectra were taken at room temperature with the film under strain. When stretched at $T < T_g^2$ (Figure 7a), despite the high deformation of the film, the two phenyl bands of azobenzene at 1500 and 1600 cm^{-1} display no dichroism within experimental errors ($A_{||} = A_{\perp}$), indicating the absence of a long-range molecular orientation of azobenzene groups inside the glassy microdomains of Azo-SCLCP. For SBS under high deformation, it is known, from small-angle X-ray scattering studies by Hashimoto and co-workers,[24,25] that short glassy cylinders of PS microdomains, which support the extension of rubbery PB chains, can be ordered with their cylindrical axes inclined at an angle and with the interdomain vectors connecting the centers of the cylinders aligned parallel to the strain direction. In the case of the azo triblock copolymer P3, at this point it is unknown whether there is a stretching-induced ordering of glassy cylindrical microdomains of Azo-SCLCP under the used conditions. Nevertheless, Figure 7a clearly indicates that there is no mechanically induced orientation of azobenzene mesogens inside the glassy microdomains of cross-links. In other words, when stretched at $T < T_g^2$, the uniaxial deformation couples to the rubbery PnBA block and the glassy microdomains of Azo-SCLCP, but it cannot deform the glassy microdomains to align mesogenic azobenzene moieties.

By contrast, when the azo triblock copolymer is stretched at $T > T_g^2$, i.e., in the LC phases of Azo-SCLCP, LC microdomains can be deformed, leading to a long-range orientation of azobenzene mesogens inside the microdomains while still sustaining part of the chain extension of PnBA. This is indeed revealed by the polarized infrared spectra in Figure 7b, where the 1500 and 1600 cm^{-1} bands clearly display strong parallel dichroism ($A_{||} > A_{\perp}$), indicating a long-range orientation of azobenzene mesogens along the strain direction when P3 is stretched at 90 °C. As the spectra were taken with the film under strain after being cooled to room temperature, the molecular orientation of azobenzene mesogens induced by stretching at 90 °C should be preserved in the glassy state. The order parameter S calculated from Figure 7b is about 0.4, corresponding to a high degree of orientation for azobenzene mesogens.[23]

Interestingly, after the film stretched at 90 °C was allowed to relax at room temperature, infrared measurements indicated that the orientation of azobenzene mesogens in the Azo-SCLCP microdomains remained almost unchanged. Moreover, when the film was stretched again under ambient conditions, the orientation increased only slightly on deformation. Figure 8 shows the changes in orientation on redrawing for two films of P3 having different order parameters in the relaxed state (initially stretched at 90 °C to different strains). In both cases, the orientation increases slightly in a linear fashion up to 150% strain. This observation reveals an interesting feature of the azo triblock copolymers. That is, after stretching in the LC phases and cooling to ambient temperatures, a new state of thermoplastic elastomer is created, in which the glassy microdomains contain azobenzene mesogens oriented in the initial strain direction. It is also interesting to notice that the similar molecular orientation of azobenzene mesogens observed in the film stretched in the LC phase, in the relaxed state, and on redrawing at room temperature implies the absence of significant rearrangement or realignment (e.g., rotation) of the cylindrical microdomains of Azo-SCLCP upon deformation and retraction of the film. This is because it is easy to picture that if the measured average molecular orientation of azobenzene mesogens was strongly coupled to a deformation-induced ordering of the cylindrical microdomains of Azo-SCLCP, on elastic retraction of the film, the molecular orientation should be significantly randomized by rearrangement of the cylinders. The experiments rather suggest that the molecular orientation of azobenzene mesogens induced by stretching at $T > T_g^2$ was mainly the result of a direct coupling of the mechanical force with the mesogenic azobenzene groups through deformation of the microdomains of Azo-SCLCP.

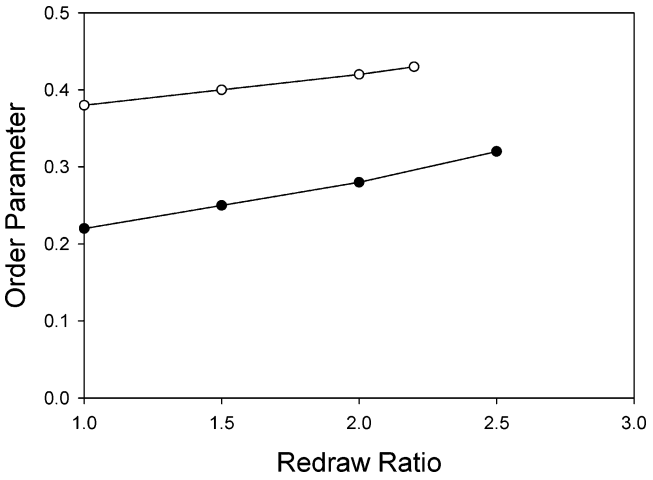

Figure 8. Order parameter of azobenzene mesogens vs redraw ratio for two films of the azo triblock copolymer P3 initially stretched at 90 °C (different strains) before cooling to and relaxation at room temperature. The order parameters prior to the redrawing represent the orientations remained in the relaxed films.

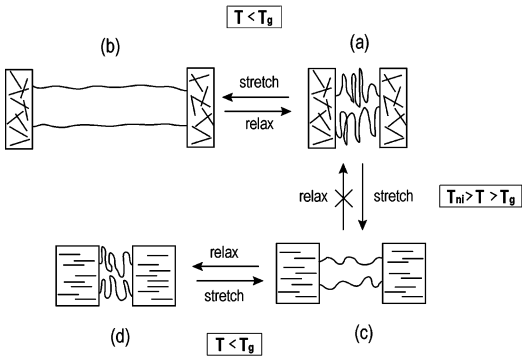

Figure 9. Schematic illustration of the elasticity and orientation states in azo triblock copolymers: (a) initial film before stretching; (b) stretching at $T < T_g$ of the azo polymer (glassy microdomains); (c) stretching at $T_{ni} > T > T_g$ of the azo polymer (liquid crystalline microdomains); and (d) relaxation at $T < T_g$ (glassy microdomains with oriented azobenzene mesogens). The elastic recovery of the film is indicated by arrows. For the sake of clarity, only rodlike azobenzene mesogens in the trans form are shown.

Figure 9 schematically illustrates, in a simplistic way, the elasticity and the orientation of azobenzene mesogens under different stretching conditions for this type of thermoplastic elastomer. In the initial film (a), there is no orientation of azobenzene mesogens inside the Azo-SCLCP microdomains connecting the rubbery chains of PnBA. Stretched at $T < T_g^2$ of the azo polymer, the normal elastic behavior is observed, with the extension

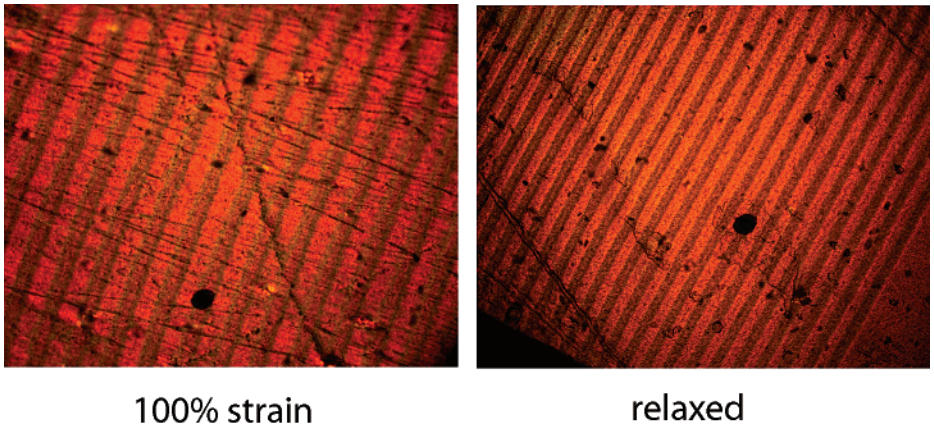

Figure 10. Polarizing optical micrographs showing a grating recorded at room temperature via a photomask (~40 μm fringes) on a film of the triblock copolymer P3 stretched to 100% deformation. The period of grating is reduced by a factor of 2 in the relaxed state. Picture area: 1070 μm × 860 μm.

of PnBA chains supported by the glassy microdomains (b), and the deformation is totally reversible. If the stretching occurs at $T_{ni} > T > T_g^2$, i.e., in the LC phases of the azo polymer, an intermediate state between the normal elastic and thermoplastic behaviors shows up (c), which is characterized by the orientation of azobenzene mesogens in the strain direction inside deformed microdomains that can still support part of chain extension of PnBA (less efficiently than glassy microdomains). If the stretched film in (c) is allowed to relax, the initial state (a) cannot be recovered (at either $T > T_g^2$ or $T < T_g^2$) because of chain relaxation of PnBA and the retaining orientation of Azo-SCLCP. Instead, after cooling to $T < T_g^2$ and partial relaxation of PnBA chains, a new relaxed state is formed (d), in which azobenzene mesogens are oriented in the initial strain direction. At $T < T_g^2$, changes between (c) and (d) are reversible.

3. Coupling between Optical and Mechanical Effects. The Azo-SCLCP used for the end blocks is the same as in the diblock copolymer with PS,[17,18] and the photoactivity arising from the reversible trans−cis isomerization of the azobenzene chromophore was also observed in the triblock copolymers. And similar to azobenzene thermoplastic elastomers prepared by grafting an Azo-SCLCP into the midblock of SBS,[13−16] coupling effects between the deformation and the photoactivity could be expected and exploited with this new azo triblock copolymer system. What follows is an example of modulating the orientation of azobenzene mesogens through the coupled effects. As discussed above, stretching a film of the azo triblock copolymer in the LC phases of Azo-SCLCP microdomains can induce a long-range orientation of azobenzene mesogens that can be retained in the film (Figure 9). If the film is subsequently exposed to UV light, either under strain or in the relaxed state, the trans−cis photoisomerization takes place, which should reduce the orientation of azobenzene mesogens. Indeed, using an oriented film of P3 under 100% strain, before exposure to UV light, the strong dichroism of the phenyl bands in the 1550−1630 cm^{-1} region gave an order parameter $S = 0.38$, indicating the orientation of azobenzene mesogens in the trans form in the strain direction. After 10 min unpolarized UV light irradiation (365 nm, 100 mW/cm^2), the dichroism diminished significantly due to the trans−cis isomerization that resulted in the loss of orientation for the isomerized azobenzene mesogens being converted to the cis form; the order parameter dropped to $S = 0.17$. The apparently incomplete randomization was mainly caused by the quite thick film used for this experiment (~16 μm under strain) for which the used UV irradiation could excite only a portion of chromophore molecules. Afterward, when the film was exposed to 10 min unpolarized visible light (440 nm, 100 mW/cm^2), no orientation recovery of azobenzene mesogens was observed in the glassy state even though the cis−trans back-isomerization took place. However, an orientation recovery was obtained by using linearly polarized visible light with the polarization perpendicular to the strain direction, with the order parameter recovered to $S = 0.27$. This orientation increase was due to the photoinduced orientation of azobenzene mesogens taking place on linearly polarized visible light irradiation after a pretreatment using unpolarized UV light.[18] Since photoalignment of azobenzene is perpendicular to the polarization of irradiation, it adds to the orientation of *trans*-azobenzene remained in the strain direction. If the polarization of the visible irradiation is parallel to the strain direction, the photoinduced orientation will be perpendicular to the mechanically induced orientation remained in the film; i.e., the film will contain biaxially oriented azobenzene mesogens. Such photoinduced changes in orientation could be repeated. Note that the elastomer films were too thick to allow polarized UV−vis spectroscopy to be used to characterize the orientation of azobenzene mesogens.

As mentioned in Introduction, one particular utility of azo thermoplastic elastomers is the possibility of recording diffraction gratings whose period, diffraction angle, and efficiency can be changed reversibly on elastic deformation of the film. For the new azo triblock copolymers studied in this work, new grating formation mechanisms may be found and are worth being exploited. The erasure of deformation-induced orientation of azobenzene mesogens in the glassy state can be used to write a grating structure. Indeed, preliminary investigations found that diffraction gratings could be formed by exposing a film with oriented azobenzene mesogens to UV light at room temperature either through a gating photomask or using an interference pattern produced by two coherent laser beams. The grating is formed as a result of the loss of orientation in irradiated areas and the remaining orientation in nonirradiated areas, which creates a refractive index modulation. Figure 10 shows the polarizing optical micrographs of a grating (period ~ 40 μm) recorded, via a photomask, on a film of P3

stretched to 100% deformation. Darker stripes are regions exposed to UV light, where the orientation of azobenzene mesogens was partly erased due to the trans−cis photoisomerization. When the film was relaxed, the period of grating diminished to about 20 μm. The changes were reversible, and the grating was stable at room temperature because the orientation lost in the glassy state could not be recovered after the thermally induced cis−trans back-isomerization of the chromophore. More studies exploring the coupling between elasticity, mesophases, and photoactivity in this new type of azo thermoplastic elastomers are underway.

Conclusions

We have prepared a new type of azobenzene-containing thermoplastic elastomers that is ABA triblock copolymer. The end blocks (A block) are a polymethacrylate-based Azo-SCLCP having a relatively high T_g, while the midblock (B block) is the low-T_g PnBA. ATRP was found to be effective to produce azo triblock copolymers with the same PnBA midblock but various degrees of polymerization for the end blocks of Azo-SCLCP. The appropriate T_g's and the thorough microphase separation between PnBA and Azo-SCLCP make the azo triblock copolymers behave like thermoplastic elastomers, whose films can readily be obtained by solution-casting or spin-coating. The elasticity coupled to the LC phases of the Azo-SCLCP forming the microdomains and the photoactivity of azobenzene mesogens related to the reversible trans−cis photoisomerization impart new features and properties to this type of thermoplastic elastomers. In particular, as compared to conventional systems such as SBS, between the normal elastic ($T_g^{PB} < T < T_g^{PS}$) and thermoplastic ($T > T_g^{PS}$) regimes, an intermediate state exists for the azo triblock copolymers. That is, when stretched at $T_{ni} > T > T_g$ of Azo-SCLCP, a long-range orientation of azobenzene mesogens can be induced inside deformed LC microdomains that can still support part of the elastic extension of PnBA chains. This molecular orientation of azobenzene can be retained in relaxed films at ambient temperatures, resulting in thermoplastic elastomers containing glassy microdomains with oriented mesogens. Moreover, the trans−cis photoisomerization of azobenzene can be used to change the orientation in the glassy state, which makes it possible to record mechanically tunable diffraction gratings using photomasks or interference patterns of two laser beams.

Acknowledgment. Financial support from the Natural Sciences and Engineering Research Council of Canada and le Fonds québécois de la recherche sur la nature et les technologies of Québec is also acknowledged.

References and Notes

(1) See recent reviews. (a) Natansohn, A.; Rochon, P. *Chem. Rev.* **2002**, *102*, 4139. (b) Ikeda, T. *J. Mater. Chem.* **2003**, *13*, 2037.
(2) Viswanathan, N. K.; Kim, D. Y.; Bian, S.; Williams, J.; Liu, W.; Li, L.; Samuelson, L.; Kumar, J.; Tripathy, S. K. *J. Mater. Chem.* **1999**, *9*, 1941.
(3) Rasmussen, P. H.; Ramanujam, P. S.; Hvilsted, S.; Berg, R. H. *J. Am. Chem. Soc.* **1999**, *121*, 4738.
(4) Eich, M.; Wendorff, J. H. *Makromol. Chem. Rapid Commun.* **1987**, *8*, 59.
(5) Wu, Y.; Zhang, Q.; Kanazawa, A.; Shiono, T.; Ikeda, T.; Nagase, Y. *Macromolecules* **1999**, *32*, 2, 3951.
(6) Fischer, T.; Lasker, L.; Stumpe, J.; Kostromin, S. *Photochem. Photobiol. A: Chem.* **1994**, *80*, 453.
(7) Han, M.; Ichimura, K. *Macromolecules* **2001**, *34*, 82.
(8) Mao, G.; Wang, J.; Clingman, S. R.; Ober, C. K.; Chen, J. T.; Thomas, E. L. *Macromolecules* **1997**, *30*, 2556.
(9) Tian, Y.; Watanabe, K.; Kong, X.; Abe, J.; Iyoda, T. *Macromolecules* **2002**, *35*, 3739.
(10) Junge, D. M.; McGrath, D. V. *J. Am. Chem. Soc.* **1999**, *121*, 4912.
(11) Li, M.-H.; Keller, P.; Li, B.; Wang, X.; Brunet, M. *Adv. Mater.* **2003**, *15*, 569.
(12) Yu, Y.; Nakano, M.; Ikeda, T. *Nature (London)* **2003**, *425*, 145.
(13) Bai, S.; Zhao, Y. *Macromolecules* **2001**, *34*, 9032.
(14) Bai, S.; Zhao, Y. *Macromolecules* **2002**, *35*, 9657.
(15) Zhao, Y.; Bai, S.; Dumont, D.; Galstian, T. *Adv. Mater.* **2002**, *14*, 512.
(16) Zhao, Y.; Bai, B.; Asatryan, K.; Galstian, T. *Adv. Funct. Mater.* **2003**, *13*, 781.
(17) Cui, L.; Zhao, Y.; Yavrian, A.; Galstian, T. *Macromolecules* **2003**, *36*, 8246.
(18) Tong, X.; Cui, L.; Zhao, Y. *Macromolecules* **2004**, *37*, 3101.
(19) Moineau, C.; Minet, M.; Teyssié, P.; Jérome, R. *Macromolecules* **1999**, *32*, 8277.
(20) Ringsdorf, H.; Schmidt, H. W. *Makromol. Chem.* **1984**, *185*, 1327.
(21) Ciampolinim, M.; Nardi, N. *Inorg. Chem.* **1966**, *5*, 41.
(22) Walther, M.; Faulhammer, H.; Kinkelmann, H. *Macromol. Chem. Phys.* **1998**, *199*, 223.
(23) Zhao, Y.; Roche, P.; Yuan, G. *Macromolecules* **1996**, *13*, 4619.
(24) Pakula, T.; Saijo, K.; Kawai, H.; Hashimoto, T. *Macromolecules* **1985**, *18*, 1294.
(25) Pakula, T.; Saijo, K.; Hashimoto, T. *Macromolecules* **1985**, *18*, 2037.

MA048995J